

Supporting Information

# Multifunctional Halloysite Nanotubes-Polydopamine Agro-Carriers for Controlling Bacterial Soft Rot Disease

*Sandeep Sharma<sup>‡</sup>, Ofer Prinz Setter<sup>‡</sup>, Hanan Abu Hamad, and Ester Segal\**

Faculty of Biotechnology and Food Engineering, Technion – Israel Institute of Technology, Haifa  
- 3200003, Israel

<sup>‡</sup> Authors contributed equally to this work

\* Corresponding author, [esegal@technion.ac.il](mailto:esegal@technion.ac.il)

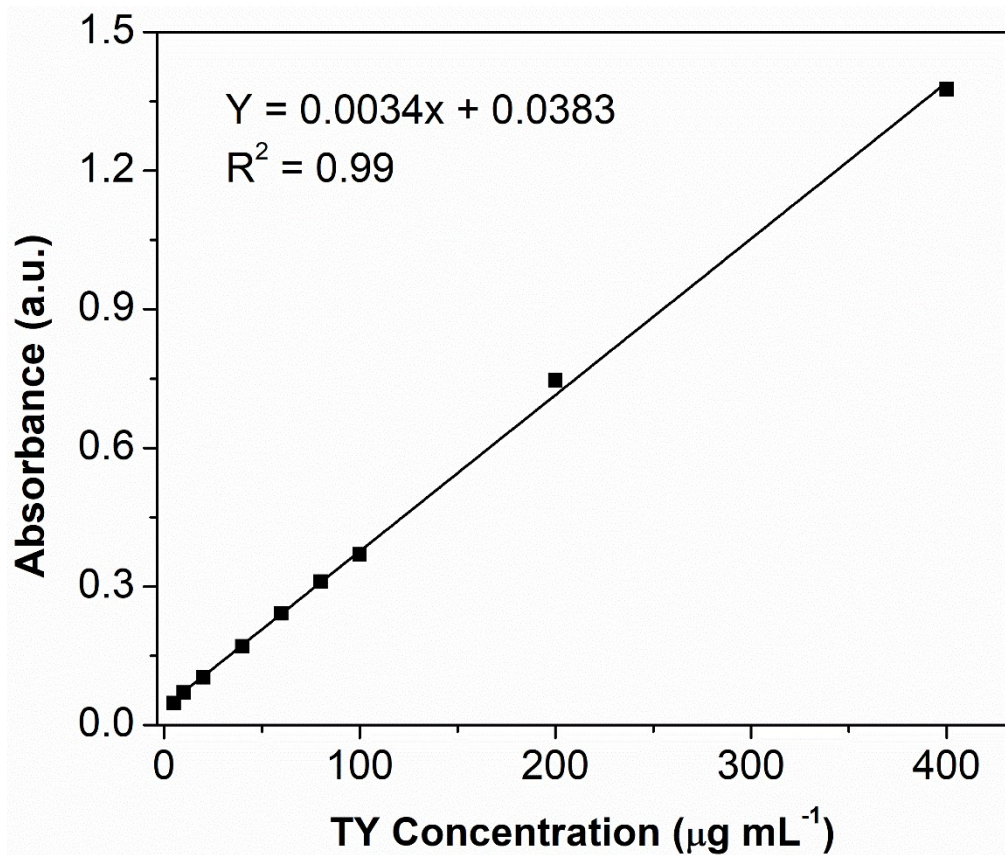


**Figure S1.** Standard curve for the absorbance of thymol (TY) solutions in ethanol at 278 nm.

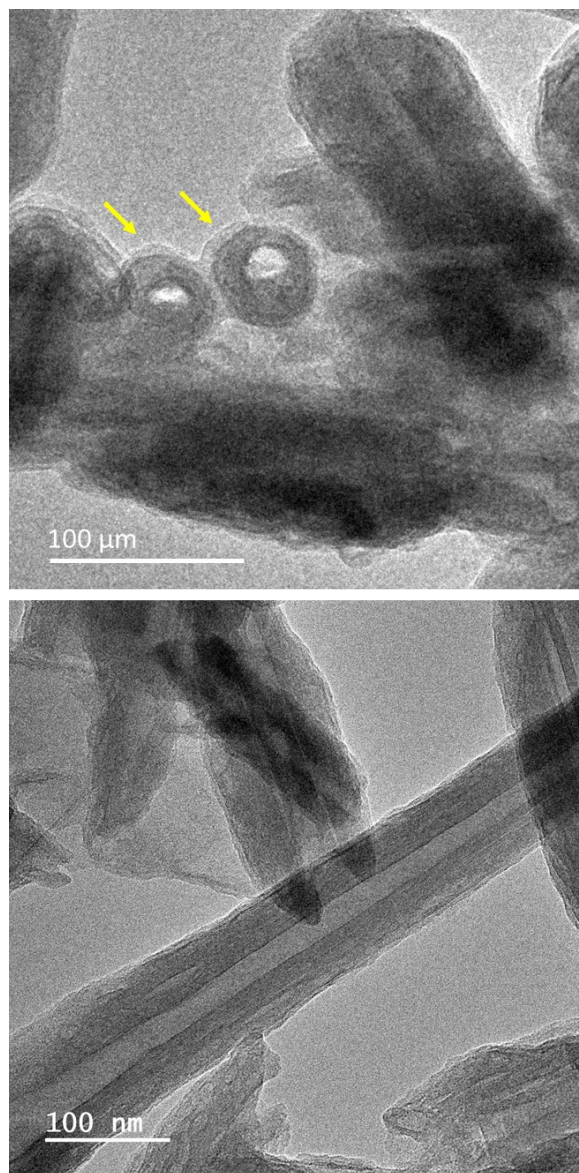


**Figure S2.** Additional high-resolution TEM images of PDA-coated HNTs. Yellow arrows indicate the PDA layer around HNTs facing the electron source with their open tube ends.

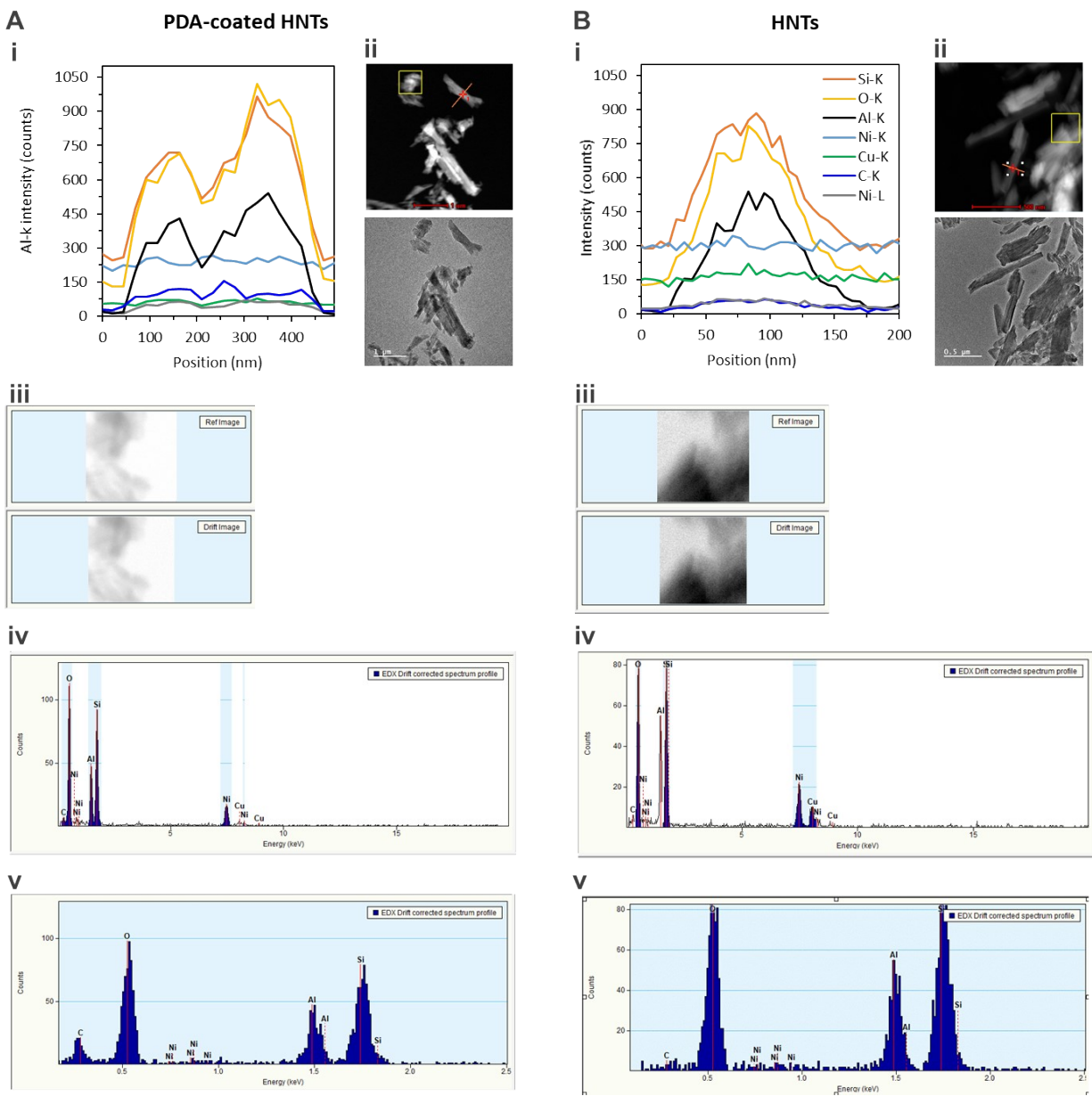


**Figure S3.** STEM-EDX Elemental profiling of (A) PDA-Coated HNTs and (B) HNTs. (i) Intensity profiles for all elements detected in the sample, including: Si (Red), O (Yellow), Al (Black), Ni (Light Blue and Gray for K and L electron shells, respectively), Cu (Green), and C (Blue). Note that Si, O, Ni, and Cu are expected to be contributed from the nickel grid used with a silicon oxide film support. (ii) TEM images of the region of interest depicting the analyzed clay tube with the profile trace indicated in orange. The object in the yellow square is used as a reference for drift compensation, and drift verification is presented in (iii). (iv) An exemplar EDX spectrum from the middle of the profile after baseline correction and peak identification. (v) Zoomed-in view of the region of interest within the EDX spectrum.

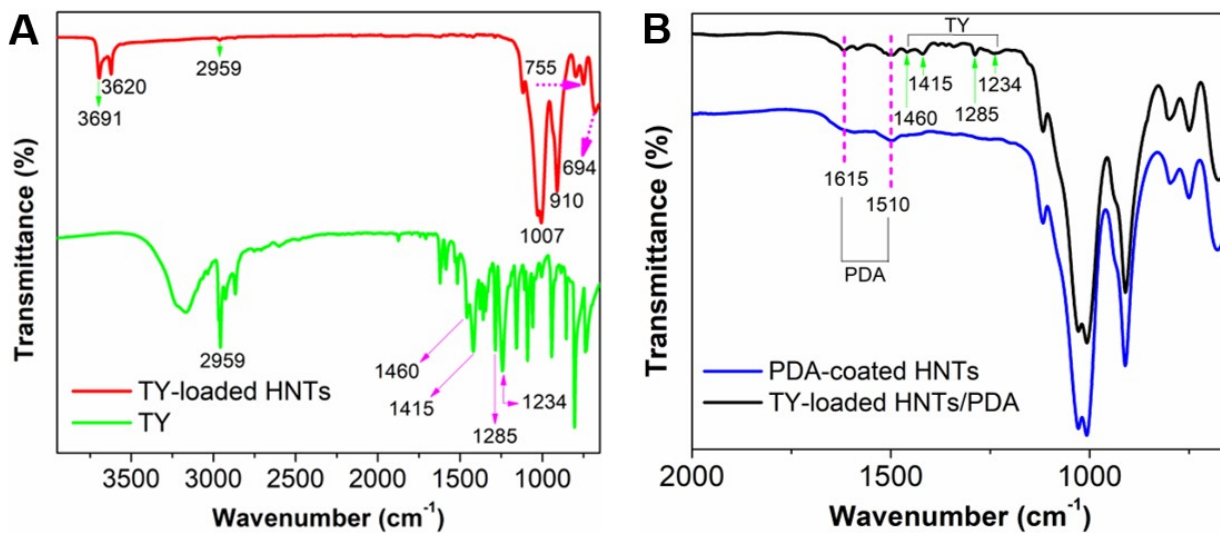


**Figure S4.** (A) FTIR spectra of TY and TY-loaded HNTs. (B) Zoom in FTIR spectra from 2000 to 600 cm<sup>-1</sup> for PDA-coated HNTs and TY-loaded HNTs/PDA hybrid.

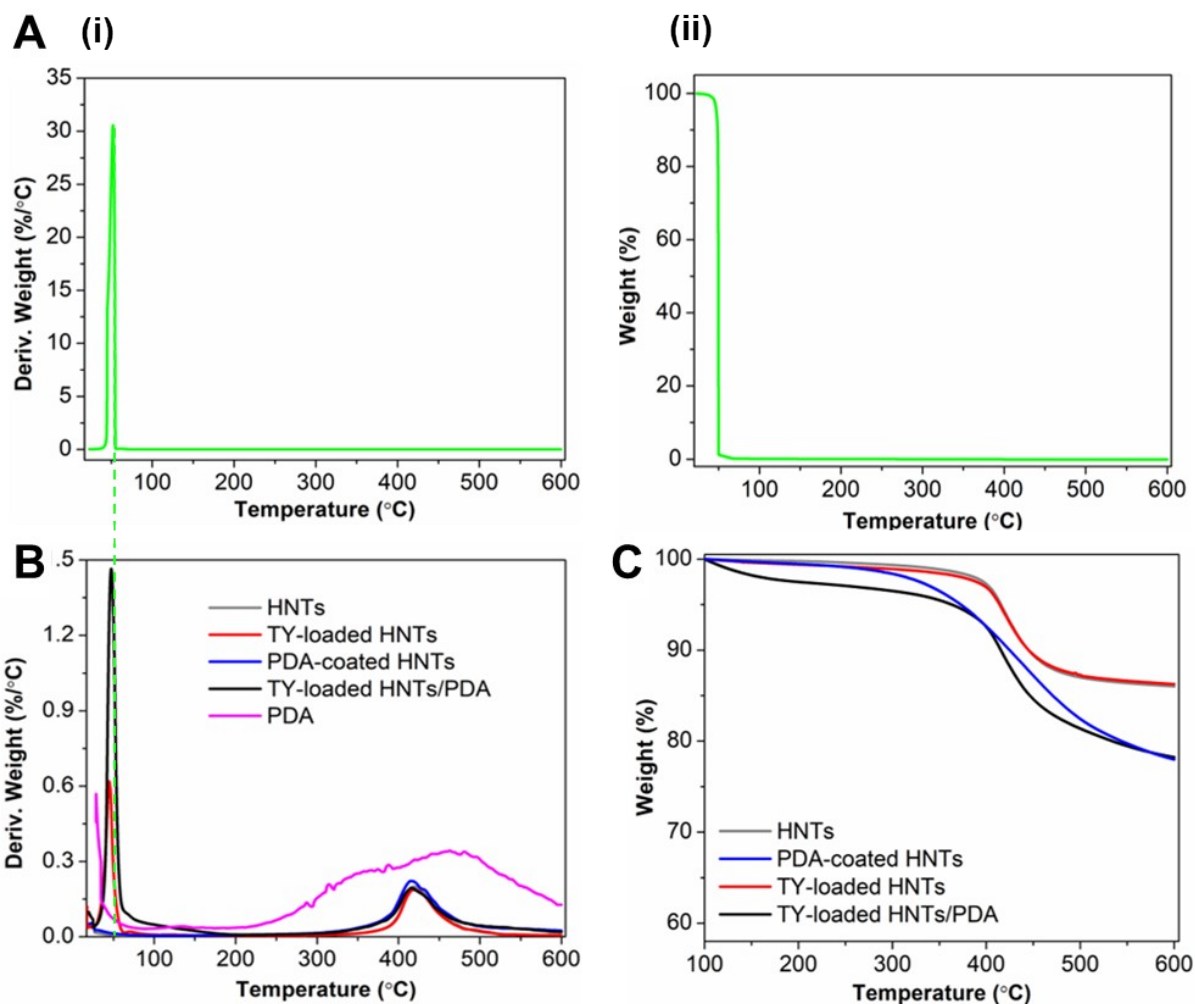


**Figure S5.** (A-i) DTG of pure thymol along with (ii) its corresponding TGA curve showing the complete evaporation of the essential up to 55 °C (indicated by the dashed green light line) oil. (B) TGA thermograms of HNTs, PDA, TY-loaded HNTs, PDA-coated HNTs, and TY-loaded HNTs/PDA hybrid. (C) Presentation of TGA curves on dry basis by normalization to mass at 100 °C for HNTs, TY-loaded HNTs, PDA-coated HNTs, and TY-loaded HNTs/PDA. (C) TGA and (D) DTG curves of TY.

**Table S1.** TY loading capacity (LC) of TY-loaded HNTs and TY-loaded HNTs/PDA hybrid calculated by TGA and multimode plate reader (Ab.).

TY-loaded HNTs/PDA		TY-loaded HNTs	
TGA	Ab.	TGA	Ab.
16.5%	14.7±1.9%	6.6%	5.6±1.8%

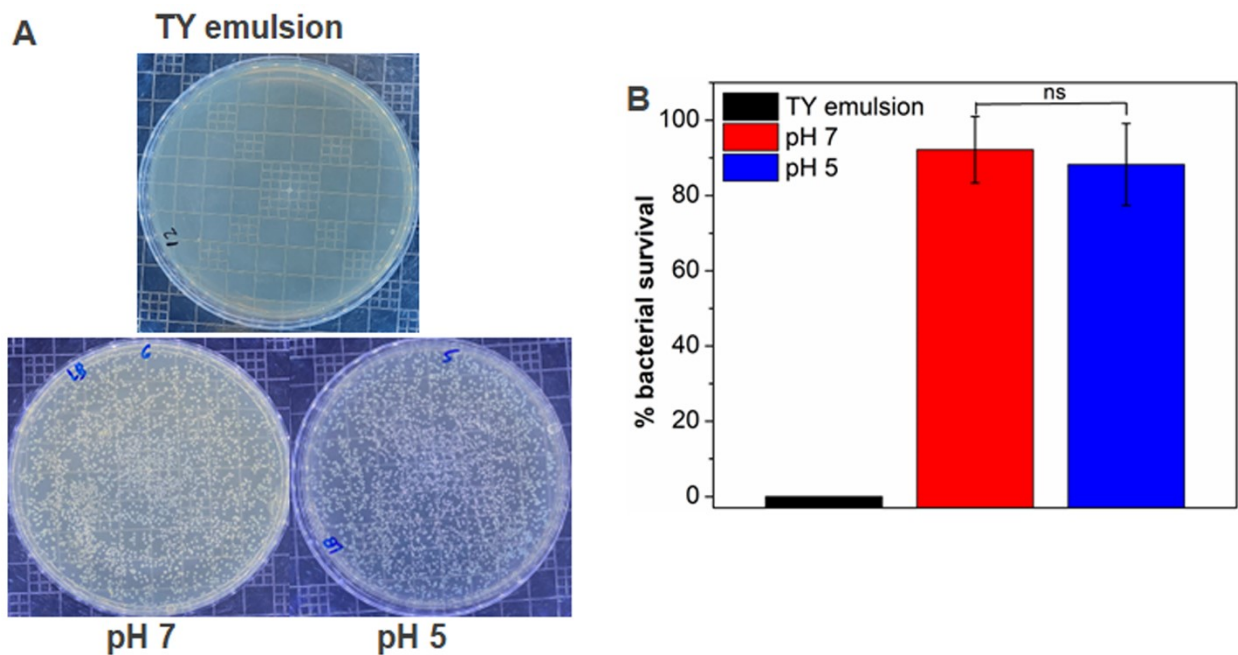


**Figure S6.** (A) Images showing the antibacterial activity of TY emulsion, as well as plain buffer solutions at pH 7 and pH 5 and (B) their corresponding % bacterial survival.

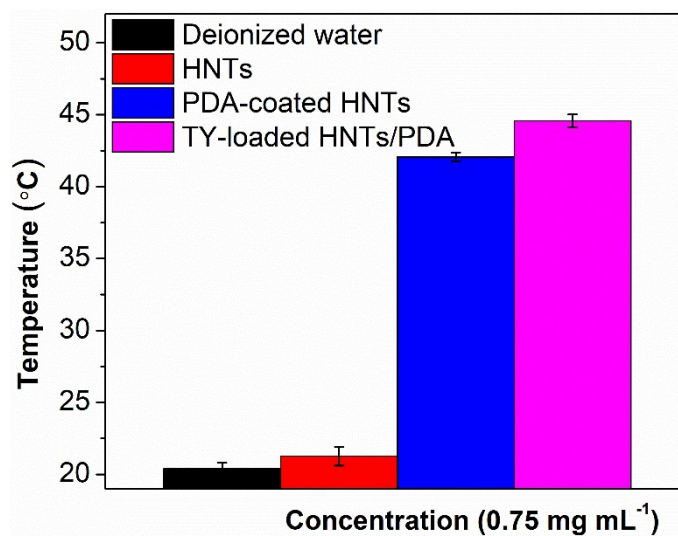


**Figure S7.** Temperature profile of deionized water, HNTs, PDA-coated HNTs, and TY-loaded HNTs/PDA hybrid after irradiation with 808 nm NIR laser for 15 minutes.

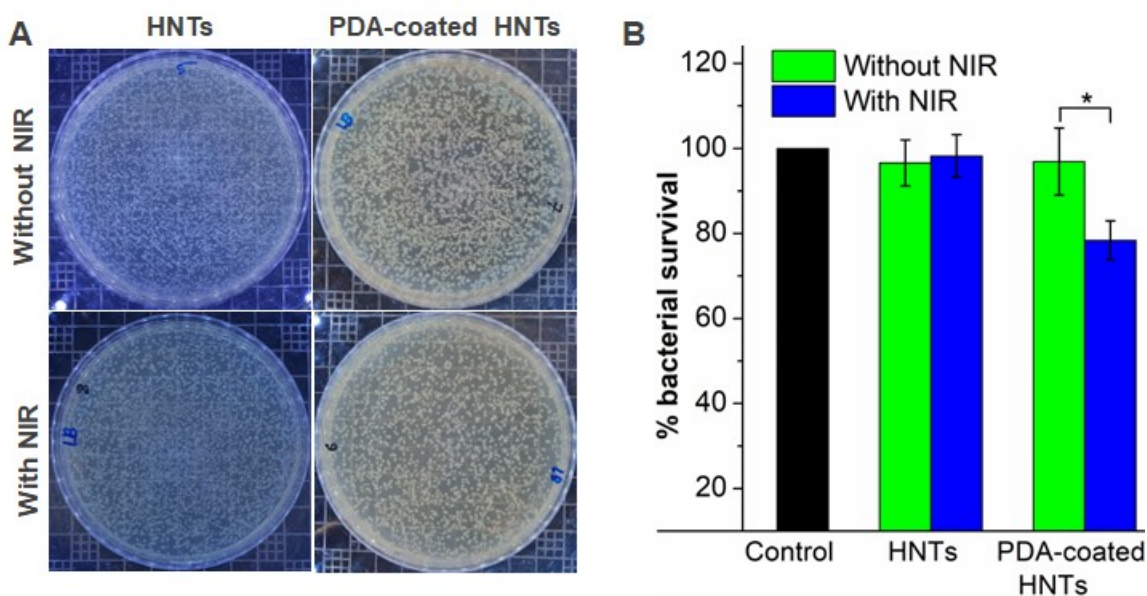


**Figure S8.** Images showing the antibacterial activity of HNTs and PDA-coated HNTs without and with irradiations with 808 nm NIR light (A) with their % bacterial survival (B).

The conjugation reaction of amino functionalized HNTs and PDA-coated HNTs with FITC involves the formation of a stable thiourea linkage between FITC and amine groups of functionalized nanotubes.<sup>1</sup> The fluorescence spectra of both FITC-conjugated HNTs and FITC-conjugated PDA-coated HNTs shows FITC emission maxima at 517 nm (SI Figure S9), which is blue shifted to 3 nm as compared to bare FITC peak (emission maxima = 520 nm), which may be due to the interactions between nanotubes and FITC. This confirms the successful conjugation of FITC to HNTs and PDA-coated HNTs.

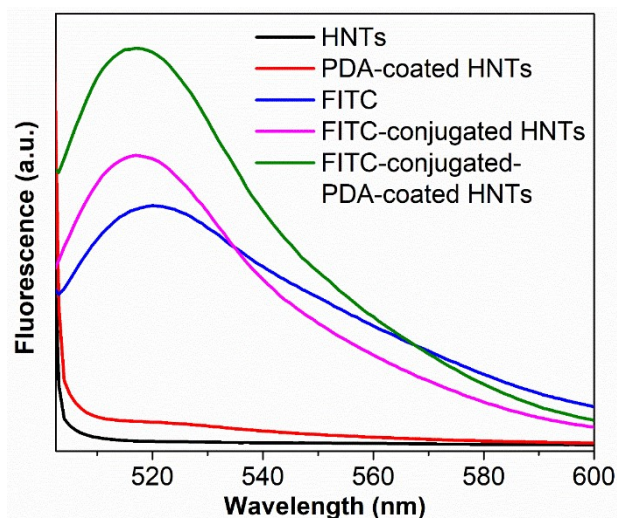


**Figure S9.** Fluorescence spectra of HNTs and PDA-coated HNTs before and after conjugation with FITC.

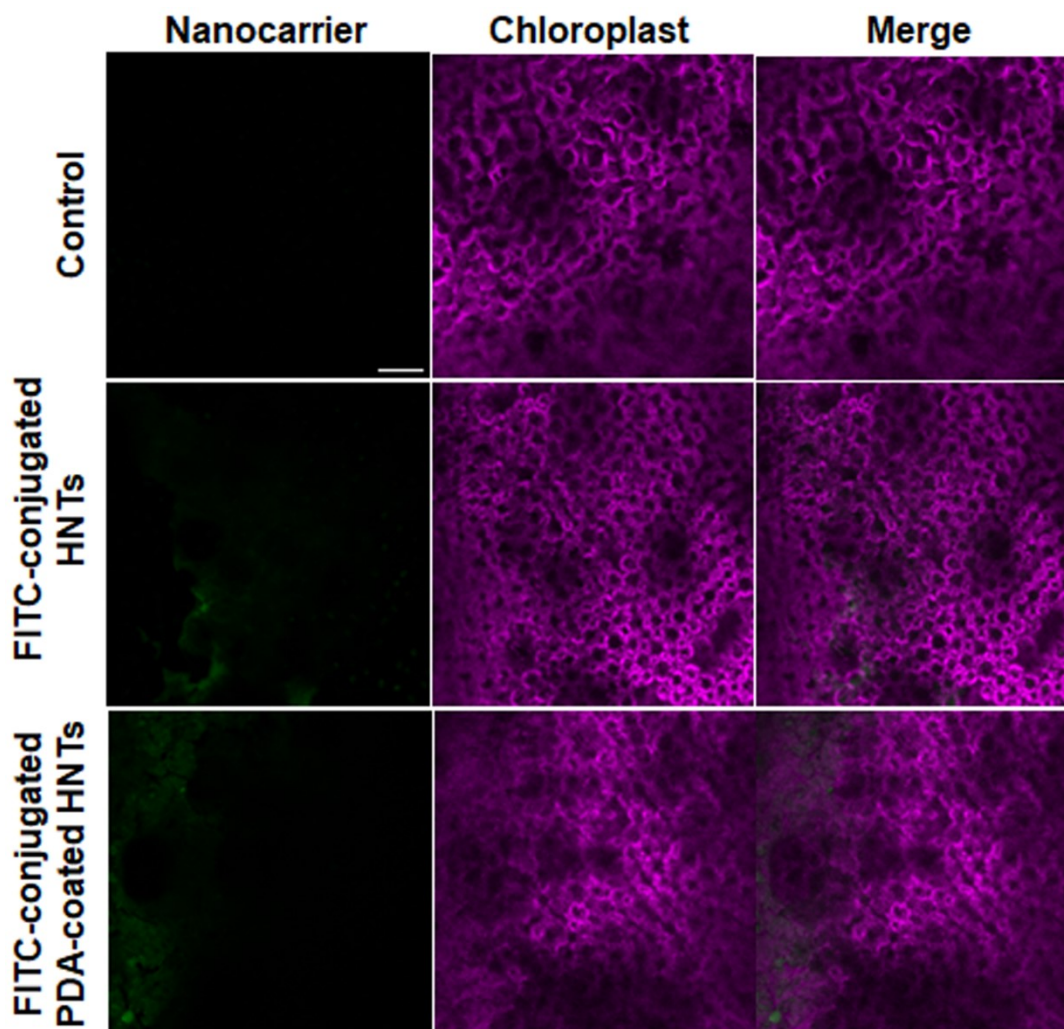


**Figure S10.** Confocal images of leaves after 24 h incubation with FITC-conjugated HNTs and FITC-conjugated PDA-coated HNTs. Green color indicates FITC fluorescence from nanotubes (Ex.  $\lambda = 488$  nm) and magenta color indicates chloroplast autofluorescence (Ex.  $\lambda = 633$  nm). Colocalization analysis (using Coloc 2) performed on the above images shows negative Pearson's coefficient ( $P = 0$ ), confirms no correlation. Scale bar = 30  $\mu\text{m}$ .

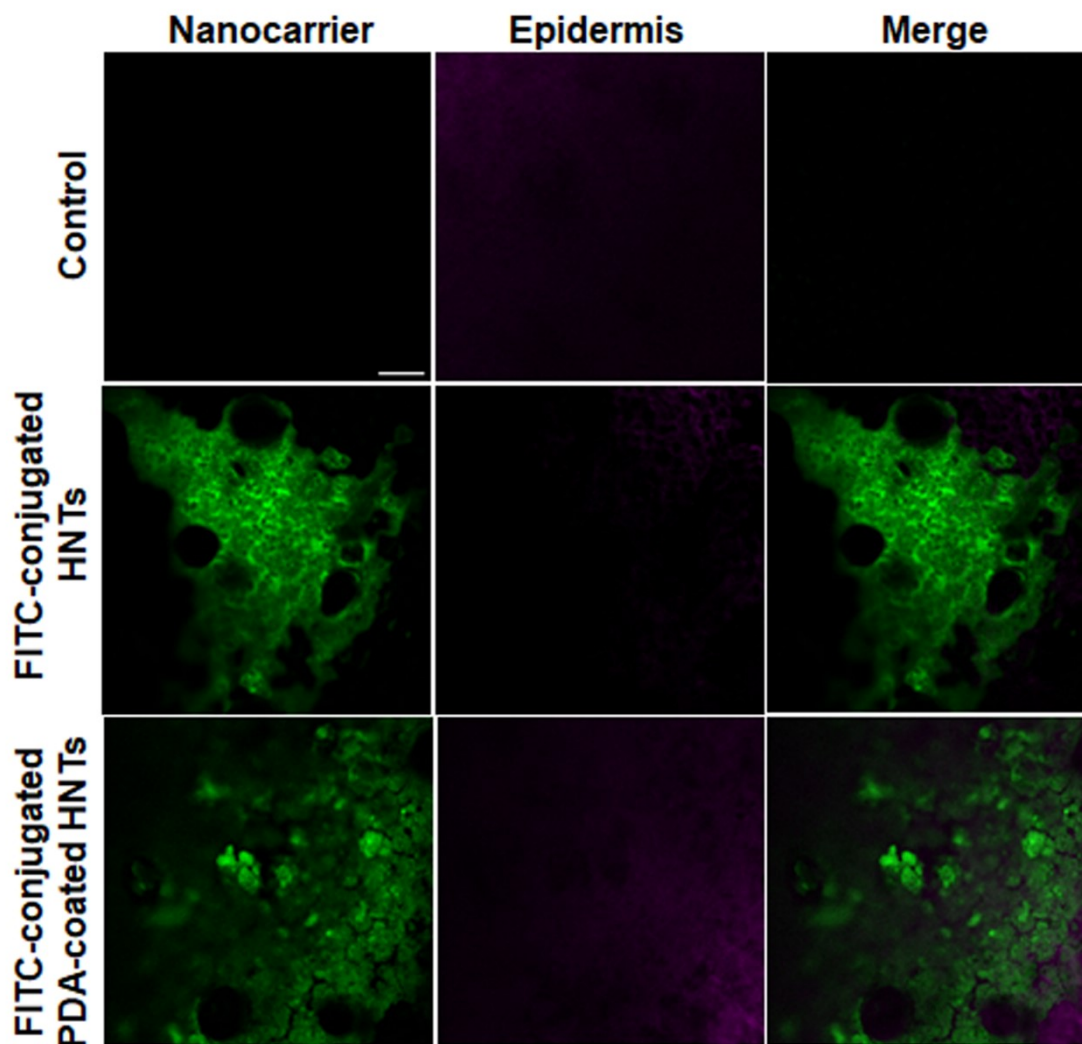


**Figure S11.** Confocal images of leaves (at epidermis surface) after 24 h incubation with FITC-conjugated HNTs and FITC-conjugated PDA-coated HNTs. Green color indicates FITC fluorescence from nanotubes (Ex.  $\lambda = 488$  nm) and magenta color indicates chloroplast autofluorescence (Ex.  $\lambda = 633$  nm). Scale bar = 30  $\mu$ m.

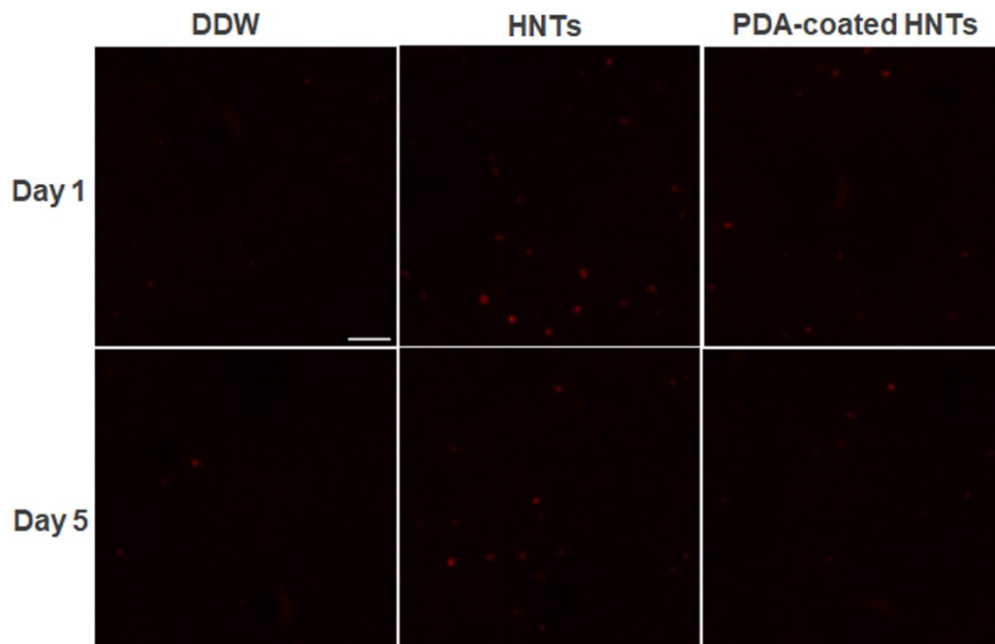


**Figure S12.** Confocal images of HNTs and PDA-coated HNTs treated leaves showing PI-stained leaf cells dead nuclei in comparison to control (DDW). Scale bar = 20  $\mu$ m.

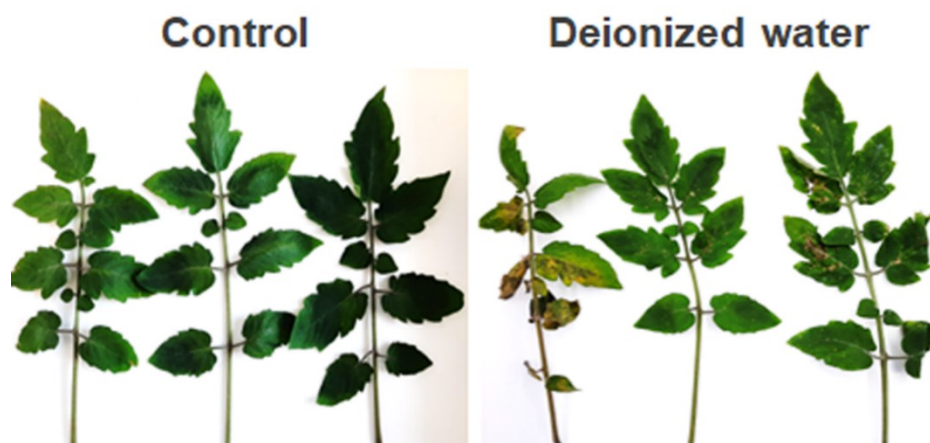


**Figure S13.** Photographs showing the uninfected (left panel) and bacterial infected leaflets (right panel) treated with deionized water.

### References

- (1) Zhao, X.; Ng, S.; Heng, B. C.; Guo, J.; Ma, L.; Tan, T. T. Y.; Ng, K. W.; Loo, S. C. J. Cytotoxicity of Hydroxyapatite Nanoparticles Is Shape and Cell Dependent. *Arch. Toxicol.* **2013**, *87* (6), 1037–1052. <https://doi.org/10.1007/S00204-012-0827-1>.